Ionization Potential, Electron Affinity, Electronegativity, Hardness, and Electron Excitation Energy: Molecular Properties from Density Functional Theory Orbital Energies

Chang-Guo Zhan, Jeffrey A. Nichols,[†] and David A. Dixon*

William R. Wiley Environmental Molecular Sciences Laboratory, Pacific Northwest National Laboratory, MS K1-83, P.O. Box 999, Richland, Washington 99352

Representative atomic and molecular systems, including various inorganic and organic molecules with covalent and ionic bonds, have been studied by using density functional theory. The calculations were done with the commonly used exchange-correlation functional B3LYP followed by a comprehensive analysis of the calculated highest-occupied and lowest-unoccupied Kohn−Sham orbital (HOMO and LUMO) energies. The basis set dependence of the DFT results shows that the economical 6-31+G* basis set is generally sufficient for calculating the HOMO and LUMO energies (if the calculated LUMO energies are negative) for use in correlating with molecular properties. The directly calculated ionization potential (IP), electron affinity (EA), electronegativity (χ), hardness (η), and first electron excitation energy (τ) are all in good agreement with the available experimental data. A generally applicable linear correlation relationship exists between the calculated HOMO energies and the experimental/calculated IPs. We have also found satisfactory linear correlation relationships between the calculated LUMO energies and experimental/calculated EAs (for the bound anionic states), between the calculated average HOMO/LUMO energies and χ values, between the calculated HOMO−LUMO energy gaps and η values, and between the calculated HOMO−LUMO energy gaps and experimental/ calculated first excitation energies. By using these linear correlation relationships, the calculated HOMO and LUMO energies can be employed to semiquantitatively estimate ionization potential, electron affinity, electronegativity, hardness, and first excitation energy.

Introduction

Density functional theory (DFT) following the approach of Kohn and Sham[1,2] has proven to be an important tool in modern quantum chemistry because of its ability to include some effects of electron correlation at a greatly reduced computational cost.[3,4,5] Within the Kohn−Sham (KS) framework of DFT, the KS orbitals are a mathematical object used to build the electron density of the chemical system. With the constructed density and the Hohenberg and Kohn theorems,[1] one can calculate a range of chemical properties of interest.

Recently, the question of the physical meaning of the KS orbitals for the exact KS functional has drawn considerable attention. Perdew et al.[6] showed for an atom of nuclear charge Z that

$$\mu = \begin{cases} -\text{IP} & (Z-1 < N < Z) \\ -\text{EA} & (Z < N < Z+1) \end{cases} \tag{1}$$

with IP the ionization potential, EA the electron affinity, N a continuous variable representing the total number of electrons, and $\mu = \partial E/\partial N$ the first derivative of the total energy (E) with respect to N, the chemical potential. Earlier, Janak proved that[7]

$$\epsilon_i = \partial E/\partial n_i \tag{2}$$

where n_i is the occupation number of the KS orbital ψ_i and ϵ_i is the corresponding KS orbital energy. On the basis of

* To whom correspondence should be addressed.
† Current address: Computer Science and Mathematics Division, Oak Ridge National Laboratory, Oak Ridge, TN 37831.

eqs 1 and 2, Perdew et al. obtained[6]

$$\epsilon_{max} = \begin{cases} -\text{IP} & (Z-1 < N < Z) \\ -\text{EA} & (Z < N < Z+1) \end{cases} \tag{3}$$

in which ϵ_{max} represents the maximum occupied KS orbital energy. This equation has been interpreted as showing that the highest occupied KS orbital energy of an N-electron system represents the negative of the exact ionization potential within exact KS density functional theory.[8−12] In subsequent work, Kleinman[13,14] argued that this was not correct and that the IP should not be exactly equal to the highest occupied molecular orbital eigenvalue. In a response to the Kleinman work, Perdew and Levy[8] showed that eq 3 holds and that this can be derived without Janak's theorem. They also clearly stated that

$$\epsilon_Z = -I_Z \, (Z-1 < N < Z)$$

and concluded that "the exact highest-occupied Kohn−Sham eigenvalue is minus the ionization energy of the Z-electron system". However, they no longer stated the relationship between EA and ϵ_Z. In fact, they stated that for an exact exchange-correlation potential there is a derivative discontinuity at $N = Z$. Because of the discontinuity of $\partial E/\partial N$, i.e. μ, eq 1 clearly shows that $\mu = -\text{IP}$ when $Z-1 < N < Z$ and $\mu = -\text{EA}$ when $Z < N < Z+1$. However, right at $N = Z$, μ takes the average value,[6] i.e., $\mu = -(\text{IP} + \text{EA})/2$. Analogously, when $Z-1 < N < Z$, ϵ_{max} in eq 3 represents the energy of one KS orbital corresponding to the HOMO of the Z-electron system, whereas when $Z < N < Z+1$, ϵ_{max} represents the energy of

Molecular Properties from DFT Orbital Energies

J. Phys. Chem. A, Vol. 107, No. 20, 2003 **4185**

another KS orbital corresponding to the LUMO of the Z-electron system or the HOMO of the $(Z + 1)$-electron system. Thus, at $N = Z$, there is a sudden change in the highest occupied KS orbital. To generalize eq 3 for the case of $N = Z$, ϵ_{max} in eq 3 must be replaced by the average of the highest-occupied KS orbital energies when $Z - 1 < N < Z$ and when $Z < N < Z + 1$ for the exact KS functional.[8] Perdew and Levy further noted that most exchange-correlation functionals are continuous approximations and cannot give the correct derivative discontinuities for integer N yielding poor orbital energies. As noted by us[15] and others,[16] there are a variety of approaches to address this problem including the use of the self-interaction correction (SIC) or optimized effective potential (OEP).

The focus of the present study is not to address the issue of the proof of the ionization potential theorem within the "exact" KS DFT, as the "exact" functional is still unknown, but to see how well a typical approximation widely used by the chemical community works. Previous work has shown that the orbital energies from practical KS DFT computations are strongly dependent on the approximation used for the exchange-correlation functional. The current work builds on our previous work where we presented a more detailed theoretical analysis of DFT orbital energies, for example, in terms of the optimized effective potential, self-interaction correction, and the asymptotic behavior of the exchange-correlation potential. Indeed, the previous work has shown that the difference between the HOMO and LUMO orbital energies corresponds more closely to the first excitation energy as compared to the difference in the ionization potential and the electron affinity. For almost all of the commonly used exchange-correlation functionals, the negative of the HOMO energy is not close to the exact IP, in contrast to the results of Hartree–Fock (HF) theory for which Koopmans' theorem is valid.[17]

Although the IP given by the negative of the DFT HOMO energy with typical exchange-correlation functionals is usually too small, it has been shown that the KS orbitals can be related to experimental IPs by a constant shift.[18] Politzer et al. showed that the experimental IPs for 9 monosubstituted benzene derivatives linearly correlate with both the HF HOMO energies and the DFT HOMO energies.[19] In addition, by comparing the KS orbital energies (ϵ_i^{KS}) with the HF orbital energies (ϵ_i^{HF}), Stowasser and Hoffman found a linear relationship for $|\epsilon_i^{KS} - \epsilon_i^{HF}|$ vs ϵ_i^{HF}.[20]

To improve the agreement of the HOMO energy with the first IP, new functionals and approximations for the KS potential have been tested which account for the effects of self-interaction,[21–23] which is ignored in all of the commonly used functionals. It has been demonstrated that, with the self-interaction correction included, the negative of the calculated HOMO energies are much closer to the corresponding first IPs and the calculated HOMO–LUMO gaps are also closer to the first electronic excitation energies. These investigations also demonstrated an excellent linear correlation between the occupied orbital energies determined by including the self-interaction correction and those determined by the commonly used functionals in which the self-interaction correction is ignored. In addition, Chong et al.[24] have performed DFT calculations by using an approximate exchange-correlation functional obtained with the "statistical average of (model) orbitals potential (SAOP)" and found that the calculated negative of the occupied KS orbitals are also close to the corresponding experimental IPs.

We are particularly interested in exploiting time-dependent DFT (TD-DFT)[25] to predict the UV–visible spectra of a wide range of molecules from new photolithographic polymers for the production of semiconductors[26] to biomolecules for neurotoxins.[27] Such TD-DFT calculations have a strong dependence on the orbital energies. We are also interested in developing computational approaches for predicting the likelihood of polymerization reactions based on the $Q-e$ scheme[28,29] and such models also require good orbital energies. The results obtained from previous investigations led us to examine whether the KS orbital energies determined by a commonly used exchange-correlation functional can be used to develop generally applicable empirical correlation relationships between the KS orbital energies and related properties. For example, if we could assume a linear relationship between the KS orbital energies determined by the "exact" KS potential and those by a commonly used exchange-correlation functional, then the KS HOMO energies calculated by using the commonly used functional could be corrected empirically to reproduce the experimental IPs. Finding such a relationship requires the ability to perform practical DFT calculations on a variety of representative chemical systems.

We focus on the HOMO and LUMO energies in order to determine if correlations with interesting molecular/atomic properties and chemical quantities exist. In simple molecular orbital theory approaches, the HOMO energy (ϵ_{HOMO}) is related to the IP by Koopmanns' theorem and the LUMO energy (ϵ_{LUMO}) has been used to estimate the electron affinity (EA). If $-\epsilon_{HOMO} \approx IP$ and $-\epsilon_{LUMO} \approx EA$, then the average value of the HOMO and LUMO energies is related to the electronegativity (χ) defined by Mulliken[30] with $\chi = (IP + EA)/2$. In addition, the HOMO–LUMO gap is related to the hardness (η)[31] and also as an approximation to the first electron excitation energy (τ). The electronegativity and hardness are of course used extensively to make predictions about chemical behavior. For example, the electronegativity is a key factor affecting the parameters Q and e in the $Q-e$ scheme[28] for the interpretation of the reactivity of a monomer containing a double bond in free-radical copolymerizations. The $Q-e$ scheme has proven to be remarkably useful and continues to be the only general reactivity scheme in use today.[32] With above definition for the electronegativity, the negative of the electronegativity is the chemical potential (μ)[33] defined as the first derivative of the total energy with respect to the number of electrons. We note that the relationship between the electronegativity and the chemical potential is in terms of the exact ionization potential and electron affinity, not in terms of an approximation for the IP and EA based on the orbital energies as usually done. A goal of this paper is to investigate how well the approximation based on orbital energies actually works. The hardness, defined as the second derivative of the total energy, together with the concept of electronegativity and the principle of equalization of electronegativities,[34–36] has been used to develop the principle of hard and soft acids and bases.[37–41] For example, hardness has also been applied to explain aromaticity in organic compounds.[42]

We have developed linear correlation relationships which can be used to semiquantitatively estimate these fundamental properties/quantities (i.e., IP, EA, χ, η, and τ) based on the calculated HOMO and LUMO energies. For comparison, in this study, we also evaluated the IP and EA by performing direct total energy calculations on the ionic systems. The appropriate use of the directly calculated IP and EA gives χ and η. A detailed comparison of the calculated results with the available experimental data shows the reliability of the developed linear correlation relationships.

Calculation Method

Geometries of all of the molecules considered in this study were fully optimized by using gradient corrected DFT with Becke's three-parameter hybrid exchange functional and the Lee–Yang–Parr correlation functional (B3LYP)[43] and with the 6-31+G* basis set.[44] Analytic second derivative calculations, which yield the harmonic vibrational frequencies, were performed at the optimized geometries to ensure that the optimized geometries are minima on the potential energy hypersurface (all real frequencies). To examine the basis set dependence of the DFT HOMO and LUMO energies, we also performed single-point energy calculations on the neutral systems using the B3LYP functional with a larger basis set, denoted by aug-cc-pVTZ+1, for all elements except Ca. Here, the notation aug-cc-pVTZ+1, as used previously, refers to the aug-cc-pVTZ correlation-consistent basis set[45] augmented with an additional set of diffuse functions (i.e., diffuse s, p, and d functions for H and diffuse s, p, d, and f functions for other elements) whose orbital exponents were determined by geometric extrapolation from the standard aug-cc-pVTZ basis set.[46] For Ca, the aug-cc-pVTZ basis set is not available, so we used the standard 6-311+G(2df) basis set[44,46] augmented with a set of diffuse s, p, d, and f functions. This augmented basis set is denoted by 6-311+G(2df)+1. The aug-cc-pVTZ+1 or 6-311+G(2df)+1 basis set was also used to perform single-point energy calculations on some of the anionic states to examine the basis set dependence of the calculated EAs. All of the B3LYP/aug-cc-pVTZ+1 (or B3LYP/6-311+G(2df)+1 for Ca) calculations were performed by using the geometries of neutral systems optimized at the B3LYP/6-31+G* level.

The energies, $E(M^+)$ and $E(M^-)$, of the ionic states of each system M were calculated at the B3LYP/6-31+G* level by using the geometry of the neutral system optimized at the B3LYP/6-31+G* level. Hence, the IP $= E(M^+) - E(M)$ and EA $= E(M) - E(M^-)$ values determined by these DFT energy calculations are the vertical ionization potential and vertical electron affinity from the bottom of the potential well of the neutral, respectively. In addition, TD-DFT calculations[25] were performed at the B3LYP/6-31+G* level to theoretically determine the first excitation energy, i.e., the lowest excitation energy, accounting for both singlet and triplet excited states. The calculated TD-DFT first excitation energy is given as τ_{TD} in the tables.

The electronegativity and hardness evaluations are all based on the commonly used finite difference approximation, leading to $\chi = (IP + EA)/2$ and $\eta = IP - EA$. Thus, with $\chi = (IP + EA)/2$ and $\eta = IP - EA$, the calculated χ and η are linear combinations of the calculated IP and EA, whereas the "experimental" χ and η are linear combinations of the experimental IP and EA.

All of the calculations were performed by using the Gaussian 98 program[47] on a 16-processor SGI Origin 2000 computer.

Results and Discussion

Basis Set Dependence of the DFT Results. Before exploring any correlation of the DFT HOMO/LUMO energies with molecular properties, we need to understand the basis set dependence of the HOMO/LUMO energies. Previous DFT calculations[15] tested a series of correlation-consistent basis sets, starting from the cc-pVTZ, and aug-cc-pVTZ basis sets and added 1 to 3 additional sets of diffuse functions (each set consists of s, p, and d shells or s, p, d, and f shells), labeled as aug-cc-pVTZ+1, aug-cc-pVTZ+2, and aug-cc-pVTZ+3. The calculated HOMO and LUMO energies indicate that the DFT results

are generally less sensitive to the basis set as compared to the corresponding Hartree–Fock (HF) calculations starting from a good quality basis set such as aug-cc-pVTZ. In the previous work,[15] orbital energies calculated with the aug-cc-pVTZ+1 basis set were reasonably well-converged in terms of the addition of more diffuse orbitals. Thus, the HOMO and LUMO energies calculated with the aug-cc-pVTZ+1 basis set can be used as a benchmark to examine whether one can use a smaller basis set, such as the 6-31+G* basis set, to obtain HOMO and LUMO energies for developing correlations with molecular properties. We note that in the previous study,[15] quite small molecules were used and there was no issue in terms of the computational resources needed, whereas we are interested in developing correlations for much larger molecular systems where a smaller basis set is needed in order to perform efficient computations.

The calculated results are collected in Tables 1 and 2 together with available experimental data. Note that the calculated vertical IP and EA values listed in the tables were determined from the total energy calculations on the neutral and ionic systems. A least-squares fit for all of the 52 systems between the $-\epsilon_{HOMO}$ values calculated using the 6-31+G* basis set and the larger basis set (LBS), i.e., the aug-cc-pVTZ+1 (or 6-311+G(2df)+1 for Ca), gave a nearly perfect linear correlation relationship

$$-\epsilon_{HOMO} = 1.001[-\epsilon_{HOMO}(LBS)] - 0.050 \text{ eV} \qquad (4)$$

with a correlation coefficient R of 0.9998 and a root-mean-square deviation (RMSD) of 0.049 eV. This correlation is given in Figure 1a. For convenience, throughout the discussion in this paper, all of the calculated results refer to those calculated at the B3LYP/6-31+G* level unless specified otherwise (with LBS in a parentheses).

As seen in Figure 1b, the correlation between the $-\epsilon_{LUMO}$ values calculated using the 6-31+G* basis set and those calculated using the larger basis set is not good when all of the 52 molecules/atoms are included. The largest difference is associated with the noble gas atom, Ne. This is not surprising as noble gases do not bind electrons. Very diffuse functions would be necessary for describing the resonant anion states of the noble gas systems, so the 6-31+G* basis set is not adequate for noble gas systems. The large difference for Ar is consistent with this result. The second largest difference is associated with H_2, and here, the difference is due to the fact that the 6-31+G* basis set for H is actually the 6-31G basis set and does not include any polarization or diffuse functions. Clearly, the 6-31G basis set is too small to correctly reproduce the LUMO energy for the hydrogen molecule. Other molecules associated with large differences in the LUMO energies include HF, H_2O, NH_3, and CH_4. Their $-\epsilon_{LUMO}$ values are calculated to be very negative (or ϵ_{LUMO} very positive) at the B3LYP/6-31+G* level, whereas the corresponding B3LYP/aug-cc-pVTZ+1 results have the opposite sign. So, the 6-31+G* basis set is insufficient for calculating the LUMO energies of these molecules. However, as clearly shown in Figure 1b, all of the calculated positive $-\epsilon_{LUMO}$ values (for 41 molecules) show an excellent linear correlation relationship

$$-\epsilon_{LUMO} = 1.0729[-\epsilon_{LUMO}(LBS)] - 0.181 \text{ eV} \qquad (5)$$

with $R = 0.991$ and RMSD $= 0.089$ eV. These results show that a small basis set can be used for calculating the LUMO energy of a molecule at the DFT level if the LUMO energy calculated using that basis set is negative. Among the 52 molecules listed in the tables, 11 molecules are estimated to

Molecular Properties from DFT Orbital Energies

J. Phys. Chem. A, Vol. 107, No. 20, 2003 **4187**

TABLE 1: Experimental and Calculated Ionization Potential (IP), Electron Affinity (EA), Electronegativity (χ = (IP + EA)/2), Hardness (η = IP − EA), First Electronic Excitation Energy (τ), Negative of HOMO Energy ($-\epsilon_{HOMO}$), Negative of LUMO Energy ($-\epsilon_{LUMO}$), Negative of Average HOMO/LUMO Energy ($-(\epsilon_{HOMO} + \epsilon_{LUMO})/2 = \chi_{HL}$), and HOMO−LUMO Energy Gap ($\epsilon_{LUMO} - \epsilon_{HOMO} = \eta_{HL}$) in eV

atom or molecule	expt[a]					calc[b]								
	IP	EA	χ	η	τ	IP	EA	χ	η	τ_{TD}	$-\epsilon_{HOMO}$	$-\epsilon_{LUMO}$	χ_{HL}	η_{HL}
1. Be	9.323				2.724	9.110	−0.232	4.439	9.342	2.105	6.285	1.373	3.829	4.912
2. Mg	7.646				2.710	7.729	−0.233	3.748	7.962	2.610	5.300	0.929	3.115	4.371
3. Ca	6.113	0.025	3.069	6.088	1.880	6.150	0.006	3.078	6.144	1.917	4.208	0.999	2.604	3.208
4. Ne	21.565				16.62	21.834	−6.831	7.502	28.665	17.388	15.691	−4.139	5.776	19.830
5. Ar	15.760				11.55	15.840	−2.630	6.605	18.470	11.098	11.663	−0.944	5.360	12.607
6. LiCl	10.01	0.59	5.30	9.42		10.050	0.717	5.383	9.333	4.251	6.887	1.690	4.289	5.197
7. LiBr	9.31	0.66	4.99	8.65		9.510	0.746	5.128	8.764	3.897	6.542	1.731	4.136	4.811
8. NaCl	9.20	0.73	4.97	8.47		9.320	0.873	5.096	8.447	3.278	6.270	2.103	4.187	4.167
9. NaBr	8.3	0.79	4.55	7.51		8.900	0.890	4.895	8.010	3.054	6.034	2.122	4.078	3.912
10. KCl	8.3	0.58	4.44	7.72		8.680	0.746	4.713	7.934	3.157	5.688	1.781	3.735	3.907
11. KBr	7.89	0.64	4.27	7.25		8.290	0.776	4.533	7.514	2.940	5.476	1.806	3.641	3.670
12. HNC	12.5					12.260	−1.299	5.481	13.559	5.666	8.980	0.040	4.510	8.940
13. HCN	13.60					13.670	−1.756	5.957	15.426	5.804	10.086	0.204	5.145	9.882
14. Li₂	5.113					5.372	0.385	2.878	4.987	0.978	3.627	1.434	2.530	2.193
15. Na₂	4.892	0.43	2.661	4.462		5.252	0.419	2.835	4.833	0.959	3.578	1.521	2.550	2.057
16. K₂	4.062	0.497	2.280	3.565		4.275	0.469	2.372	3.806	0.614	2.894	1.408	2.151	1.486
17. CO	14.104				6.3	14.230	−1.283	6.474	15.513	5.814	10.533	1.197	5.865	9.336
18. CO₂	13.773					13.838	−0.922	6.458	14.760	7.376	10.471	0.561	5.516	9.909
19. H₂	15.426				11.8	16.653	−5.771	5.441	22.424	10.582	11.809	−2.724	4.543	14.532
20. LiH	7.9	0.342	4.121	7.558	3.2	8.283	0.408	4.346	7.875	2.700	5.322	1.318	3.320	4.004
21. HF	16.03				10.3	16.278	−3.875	6.201	20.153	9.789	11.453	−0.992	5.231	12.444
22. N₂	15.581				7.8	15.841	−1.903	6.969	17.744	6.942	11.950	1.127	6.539	10.823
23. H₂O	12.621				7.1	12.700	−2.938	4.881	15.638	7.146	8.688	−0.678	4.005	9.365
24. NH₃	10.07				5.7	10.829	−2.302	4.264	13.131	6.003	7.289	−0.457	3.416	7.745
25. CH₄	14.40[c]				10.9	14.176	−1.906	6.135	16.082	9.704	10.739	−0.463	5.138	11.202
26. HC≡CH	11.400				5.2	11.276	−1.435	4.920	12.711	4.959	8.069	−0.401	3.834	8.470
27. CH₂=CH₂	10.514				4.4	10.487	−1.772	4.357	12.259	4.052	7.546	0.218	3.882	7.328
28. CH₂=CH−C(O)OH	10.60					10.723	−0.302	5.211	11.025	3.483	8.034	1.872	4.953	6.161
29. CH₂=CH−C≡N	10.91					10.689	−0.226	5.231	10.915	3.317	8.158	1.964	5.061	6.193
30. CH₂=CH−CH=CH₂	9.082					8.803	−0.846	3.979	9.649	2.771	6.520	1.095	3.807	5.424
31. CH₂=C(CN)CH₃	10.34					10.102	−0.253	4.924	10.355	3.166	7.744	1.790	4.767	5.954
32. CH₂=CH−C(O)OCH₃	9.9					10.184	−0.190	4.997	10.374	3.394	7.713	1.900	4.807	5.813
33. CH₂=C(CH₃)C(O)OCH₃	9.7					9.779	−0.513	4.633	10.292	3.374	7.487	1.470	4.478	6.018
34. C₆H₅−CH=CH₂	8.43					8.224	−0.433	3.895	8.657	2.849	6.316	1.286	3.801	5.030
35. CH₃C(O)O−CH=CH₂	9.19					9.559	−1.119	4.220	10.678	3.862	7.130	0.791	3.961	6.339
36. CH₂=CHCl	9.99					9.966	−1.415	4.275	11.381	3.863	7.363	0.594	3.978	6.770
37. CH₂=CCl₂	9.79					9.805	−0.975	4.415	10.780	3.673	7.432	0.947	4.190	6.485
38. CH₃CH=CH₂	9.73					9.700	−1.610	4.045	11.310	4.051	7.058	−0.099	3.480	7.158
39. CH₂=C(CH₃)₂	9.58					9.200	−1.489	3.856	10.689	3.998	6.757	−0.107	3.325	6.864
40. CH₂=C(CH₃)CH=CH₂	8.84					8.604	−0.795	3.905	9.399	2.827	6.428	1.034	3.731	5.393
41. CH₂=CH−CH=O	10.103					9.997	−0.058	4.969	10.055	3.038	7.396	2.209	4.803	5.188
42. CH₂=C(CH₃)CH=O	9.92					10.994	−0.086	5.454	11.080	3.126	7.336	2.064	4.700	5.272
43. CH₂=C(CN)₂	11.38					11.019	1.098	6.059	9.921	2.889	8.746	3.188	5.967	5.559
44. CH₂=CH−C(O)CH₃	9.64					9.567	−0.130	4.718	9.697	3.042	7.145	2.001	4.573	5.144
45. CH₃CH₂O−CH=CH₂	8.8					8.621	−1.499	3.561	10.120	3.819	6.203	−0.304	2.950	6.507
46. CH₂=CH−C(O)NH₂	9.5					9.798	−0.585	4.606	10.383	3.587	7.240	1.403	4.322	5.837
47. CH₂=CH−CH₂−OH	9.67					9.871	−1.303	4.284	11.174	4.032	7.450	0.486	3.968	6.964
48. CH₂=CH−C₅H₃N[d]	8.6					8.510	−0.231	4.139	8.741	2.887	6.564	1.543	4.053	5.022
49. CH₂=C(CH₃)C(O)OH	10.15					10.066	−0.284	4.891	10.350	3.266	7.691	1.766	4.728	5.925
50. CH₂=CH−OCH₃	8.93					8.749	−1.469	3.640	10.218	3.816	6.256	−0.254	3.001	6.510
51. CH₂=CHF	10.363					10.464	−1.627	4.418	12.091	4.133	7.532	0.190	3.861	7.343
52. CF₂=CF₂	10.12					10.537	−1.126	4.706	11.663	4.334	7.627	0.215	3.921	7.412

[a] Experimental IPs and EAs from ref 48 unless indicated otherwise. Experimental electron excitation energies from ref 15 and references therein. [b] All calculations were performed at the B3LYP/6-31+G* level. τ_{TD} corresponds to the lowest excitation, either singlet or triplet. [c] Experimental vertical ionization energy for CH₄ from ref 49. Note that for CH₄ the experimental adiabatic ionization energy of 12.61 eV (ref 48) or 12.78 eV (ref 51) is significantly lower than the corresponding experimental vertical ionization energy because its cationic structure considerably differs from the neutral structure (ref 51). [d] 2-Vinylpyridine.

have positive LUMO energies when the 6-31+G* basis set is used, whereas only 2 have slightly positive LUMO energies (0.225 eV for Ne and 0.044 eV for H₂) when the large basis set is used, suggesting that larger basis sets are needed for these molecules.

The HOMO and LUMO energies can be used to estimate the electronegativity (χ), hardness (η), and first electron excitation energy (τ) from the expressions $\chi_{HL} = -(\epsilon_{HOMO} + \epsilon_{LUMO})/2$ and $\eta_{HL} = \epsilon_{LUMO} - \epsilon_{HOMO}$ (see below for detailed discussion) where $\tau_{HL} = \eta_{HL}$. From eqs 4 and 5, one can expect satisfactory

linear correlation relationships between the χ_{HL} or η_{HL} values calculated using the smaller and larger basis sets for all of the 41 molecules whose LUMO energies are estimated to be negative at the B3LYP/6-31+G* level

$$\chi_{HL} = 0.9838\chi_{HL}(LBS) + 0.013 \text{ eV} \qquad (6)$$

with $R = 0.998$ and RMSD = 0.055 eV and

$$\eta_{HL} = 1.020\eta_{HL}(LBS) - 0.070 \text{ eV} \qquad (7)$$

TABLE 2: Electron Affinity (EA), Negative of HOMO Energy ($-\epsilon_{HOMO}$), Negative of LUMO Energy ($-\epsilon_{LUMO}$), Negative of Average HOMO/LUMO Energy ($-(\epsilon_{Homo} + \epsilon_{LUMO})/2 = \chi_{HL}$), and HOMO−LUMO Energy Gap ($\epsilon_{LUMO} - \epsilon_{Homo} = \eta_{HL}$) in EV Calculated at the B3LYP/Aug-cc-pVTZ+1//B3LYP/6-31+G*, or B3LYP/6-311+G(2df)+1//B3LYP/6-31+G* for Ca, Level

atom or molecule	EA calc.	EA expt.[a]	$-\epsilon_{HOMO}$ calc.	$-\epsilon_{LUMO}$ calc.	χ_{HL} calc.	η_{HL} calc.
1. Be			6.320	1.417	3.868	4.903
2. Mg			5.296	0.920	3.108	4.376
3. Ca	0.108	0.025	4.196	1.026	2.611	3.169
4. Ne			15.663	−0.225	7.719	15.889
5. Ar			11.682	0.101	5.891	11.580
6. LiCl	0.685	0.59	6.902	1.641	4.271	5.261
7. LiBr	0.729	0.66	6.571	1.716	4.143	4.855
8. NaCl	0.848	0.73	6.287	2.061	4.174	4.226
9. NaBr	0.876	0.79	6.076	2.106	4.091	3.970
10. KCl	0.669	0.58	5.798	1.689	3.743	4.110
11. KBr	0.717	0.64	5.584	1.753	3.668	3.831
12. HNC			9.050	0.515	4.782	8.536
13. HCN			10.146	0.416	5.281	9.730
14. Li$_2$	0.415		3.593	1.438	2.516	2.155
15. Na$_2$	0.429	0.43	3.556	1.507	2.531	2.048
16. K$_2$	0.494	0.497	2.895	1.425	2.160	1.469
17. CO			10.551	1.219	5.885	9.332
18. CO$_2$			10.461	0.694	5.577	9.767
19. H$_2$			11.812	−0.044	5.884	11.855
20. LiH	0.446	0.342	5.232	1.366	3.299	3.866
21. HF			11.495	0.790	6.143	10.705
22. N$_2$			11.961	1.105	6.533	10.856
23. H$_2$O			8.799	0.730	4.765	8.069
24. NH$_3$			7.429	0.561	3.995	6.867
25. CH$_4$			10.752	0.317	5.535	10.435
26. HC≡CH			8.201	0.170	4.185	8.031
27. CH$_2$=CH$_2$			7.655	0.368	4.012	7.287
28. CH$_2$=CH−C(O)OH			8.021	1.953	4.987	6.068
29. CH$_2$=CH−C≡N			8.221	2.063	5.142	6.158
30. CH$_2$=CH−CH=CH$_2$			6.605	1.207	3.906	5.398
31. CH$_2$=C(CN)CH$_3$			7.800	1.886	4.843	5.914
32. CH$_2$=CH−C(O)OCH$_3$			7.743	1.976	4.860	5.766
33. CH$_2$=C(CH$_3$)C(O)OCH$_3$			7.537	1.546	4.541	5.991
34. C$_6$H$_5$−CH=CH$_2$			6.390	1.398	3.894	4.991
35. CH$_3$C(O)O−CH=CH$_2$			7.175	0.860	4.018	6.315
36. CH$_2$=CHCl			7.414	0.728	4.071	6.686
37. CH$_2$=CCl$_2$			7.456	1.063	4.260	6.393
38. CH$_3$CH=CH$_2$			7.139	0.301	3.720	6.838
39. CH$_2$=C(CH$_3$)$_2$			6.841	0.389	3.615	6.453
40. CH$_2$=C(CH$_3$)CH=CH$_2$			6.521	1.148	3.834	5.373
41. CH$_2$=CH−CH=O			7.401	2.278	4.840	5.123
42. CH$_2$=C(CH$_3$)CH=O			7.346	2.130	4.738	5.215
43. CH$_2$=C(CN)$_2$	1.1810		8.790	3.262	6.026	5.528
44. CH$_2$=CH−C(O)CH$_3$			7.162	2.067	4.614	5.095
45. CH$_3$CH$_2$O−CH=CH$_2$			6.322	0.374	3.348	5.949
46. CH$_2$=CH−C(O)NH$_2$			7.291	1.626	4.459	5.664
47. CH$_2$=CH−CH$_2$−OH			7.494	0.600	4.047	6.894
48. CH$_2$=CH−C$_5$H$_3$N[b]			6.640	1.653	4.146	4.987
49. CH$_2$=C(CH$_3$)C(O)OH			7.747	1.841	4.794	5.906
50. CH$_2$=CH−OCH$_3$			6.378	0.362	3.370	6.016
51. CH$_2$=CHF			7.615	0.340	3.977	7.275
52. CF$_2$=CF$_2$		CF$_2$=CF$_2$	7.575	0.498	4.037	7.077

[a] Experimental EAs from ref 48. Experimental electron excitation energies from ref 15 and references therein. [b] 2-Vinylpyridine.

with $R = 0.999$ and RMSD = 0.095 eV. It is not surprising that the correlations become worse if the 11 molecules with positive LUMO energies are included in the fits as shown in Figure 1, parts c and d. The excellent linear relationships eqs 4−7 clearly indicate that it does not matter whether the $-\epsilon_{HOMO}$, $-\epsilon_{LUMO}$, χ_{HL}, and η_{HL} values calculated by using the 6-31+G* basis set or those calculated by using the larger basis set are used for exploring possible correlations with molecular properties for the molecules whose LUMO energies calculated with the 6-31+G* basis set are negative.

The calculated EAs are expected to be much more sensitive to the basis set than the corresponding IPs. For the neutral molecules considered in this study, the EA is related to the anionic system whose electron charge distribution becomes much more diffuse and requires the use of a larger basis set (usually including at least one set of diffuse functions), whereas the IP is related to a cationic system. We expect that the 6-31+G* basis set is adequate for predicting the IPs of neutral molecules as confirmed by their agreement with the corresponding experimental data (see Table 1) but is probably too small to predict EAs for a number of molecules. As shown in Table 1, the DFT calculations at the B3LYP/6-31+G* level predict that only 12 of the 52 molecules are associated with positive EAs, whereas the other 40 anions are predicted to be unbound. These 12 EA values are all close to the corresponding EAs (Table 2) calculated by using the larger basis set. As shown in
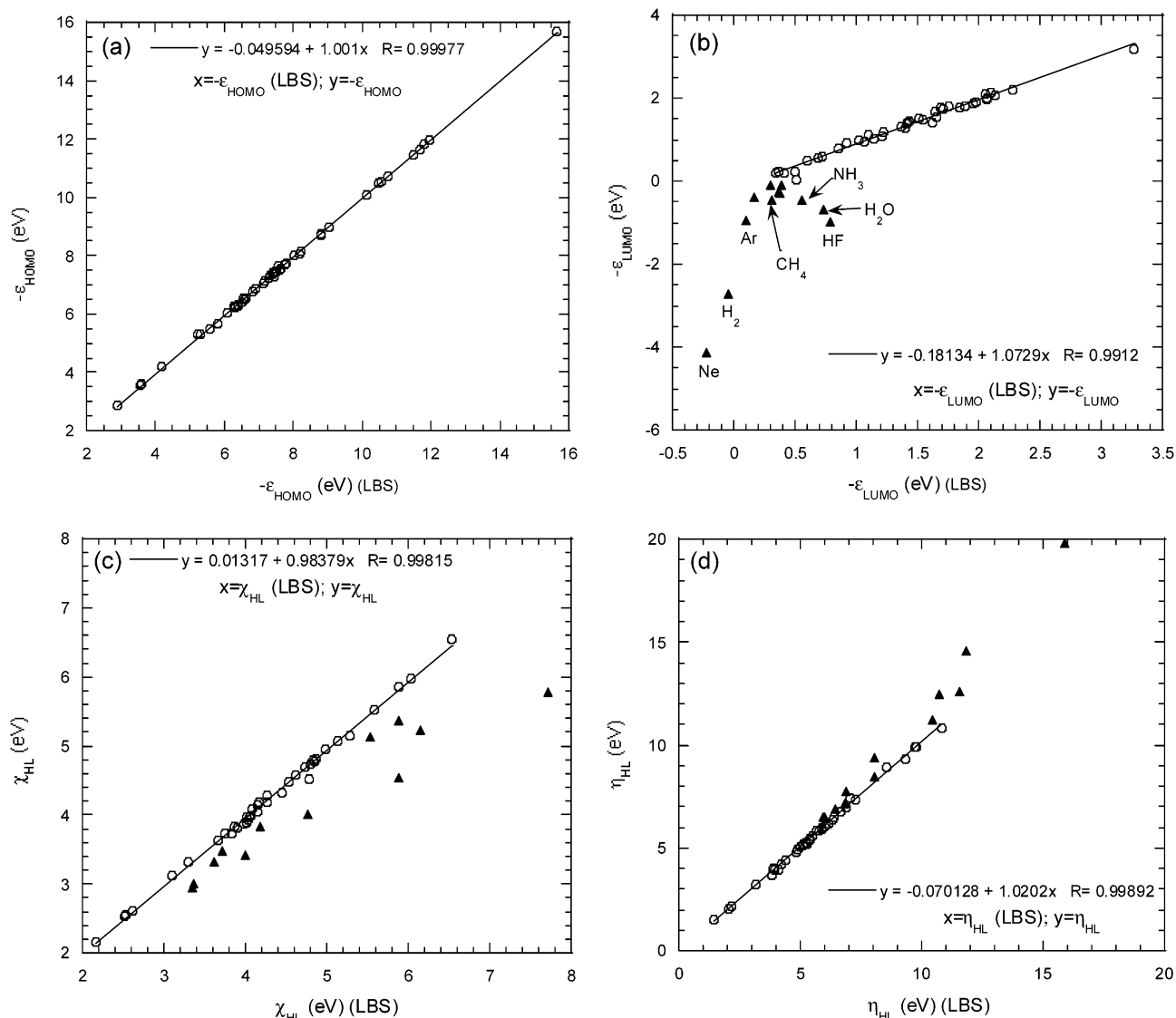
Molecular Properties from DFT Orbital Energies

J. Phys. Chem. A, Vol. 107, No. 20, 2003 **4189**

Figure 1. Plot of the $-\epsilon_{HOMO}$ (a), $-\epsilon_{LUMO}$ (b), χ_{HL} (c), and η_{HL} (d) values calculated using the 6-31+G* basis set versus those calculated using the larger basis set (LBS). The circles and solid triangles refer to the data associated with the positive and negative $-\epsilon_{LUMO}$ (6-31+G*) values, respectively.

Figure 2, we obtained a satisfactory linear relationship between these two sets of EA values

$$EA_{calc} = 1.0557 EA_{calc}(LBS) - 0.041 \text{ eV} \qquad (8)$$

with $R = 0.985$ and RMSD = 0.049 eV. In addition, we also tested the B3LYP/aug-cc-pVTZ+1 calculations on some of the unbound anions to examine the calculated negative EAs. For the anions examined, the EAs predicted at the B3LYP/aug-cc-pVTZ+1 level have the same signs as the corresponding EAs predicted at the B3LYP/6-31+G* level, but the magnitudes of the calculated negative EAs are significantly reduced, and we found no satisfactory linear correlation between the two sets of negative EA values. So, our discussion of the correlation about EAs must be limited to the positive EA values corresponding to bound anionic states.

Ionization Potential. We have collected in Table 1 a total of 52 representative molecular/atomic systems for which the experimental IP[48−51] is available, including various inorganic and organic molecules and including compounds with covalent and ionic bonds. A survey of Table 1 reveals that the directly calculated vertical IPs are, on the whole, in good agreement with the corresponding experimental IPs, but the negatives of
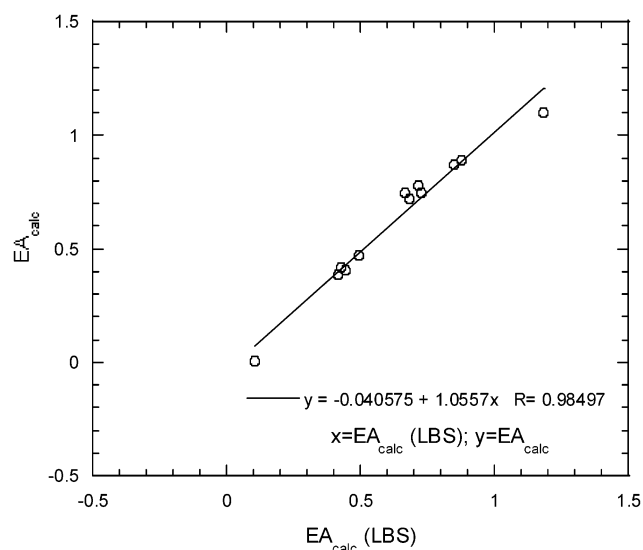

Figure 2. Plot of the electron affinities calculated using the 6-31+G* basis set versus those calculated using the larger basis set.

the HOMO energies, i.e., $-\epsilon_{HOMO}$, calculated with both the smaller and larger basis sets are all systematically smaller than

TABLE 3: Comparison of the Experimental Data[a] with the Results (All in eV) Calculated by Using the Empirical Linear Relationships eqs 7, 10, 13, 16, and 19 for Ionization Potential (IP), Electron Affinity (EA), Electronegativity (χ), Hardness (η), and First Electronic Excitation Energy (τ)

atom or molecule	IP calc.	IP expt.	EA calc.	EA expt.	χ calc.	χ expt.	η calc.	η expt.	τ calc.	τ expt.
1. Be	8.666	9.323							3.103	2.724
2. Mg	7.383	7.646							2.602	2.710
3. Ca	5.961	6.113	0.133	0.025	2.923	3.069	6.370	6.088	1.524	1.880
4. Ne	20.915	21.565							16.931	16.62
5. Ar	15.670	15.760							10.236	11.55
6. LiCl	9.450	10.01	0.554	0.59	5.148	5.30	9.575	9.42		
7. LiBr	9.000	9.31	0.579	0.66	4.946	4.99	8.953	8.65		
8. NaCl	8.646	9.20	0.806	0.73	5.013	4.97	7.915	8.47		
9. NaBr	8.339	8.30	0.817	0.79	4.869	4.55	7.504	7.51		
10. KCl	7.888	8.30	0.609	0.58	4.416	4.44	7.496	7.72		
11. KBr	7.612	7.89	0.625	0.64	4.292	4.27	7.115	7.25		
12. HNC	12.175	12.5								
13. HCN	13.616	13.60								
14. Li$_2$	5.204	5.113								
15. Na$_2$	5.140	4.892	0.451	0.43	2.851	2.661	4.516	4.462		
16. K$_2$	4.250	4.062	0.382	0.497	2.324	2.280	3.596	3.565		
17. CO	14.198	14.104							7.204	6.3
18. CO$_2$	14.117	13.773								
19. H$_2$	15.860	15.426							12.020	11.8
20. LiH	7.412	7.9	0.327	0.342	3.868	4.121	7.653	7.558	2.261	3.2
21. HF	15.396	16.03							10.085	10.3
22. N$_2$	16.043	15.581							8.582	7.8
23. H$_2$O	11.795	12.6							7.231	7.1
24. NH$_3$	9.973	10.07							5.729	5.7
25. CH$_4$	14.466	14.40[b]							8.933	10.9
26. HC≡CH	10.989	11.400							6.401	5.2
27. CH$_2$=CH$_2$	10.313	10.514							5.342	4.4
28. CH$_2$=CH−C(O)OH	10.943	10.60								
29. CH$_2$=CH−C≡N	11.105	10.91								
30. CH$_2$=CH−CH=CH$_2$	8.972	9.082								
31. CH$_2$=C(CN)CH$_3$	10.566	10.34								
32. CH$_2$=CH−C(O)OCH$_3$	10.525	9.9								
33. CH$_2$=C(CH$_3$)C(O)OCH$_3$	10.231	9.7								
34. C$_6$H$_5$−CH=CH$_2$	8.706	8.43								
35. CH$_3$C(O)O−CH=CH$_2$	9.766	9.19								
36. CH$_2$=CHCl	10.070	9.99								
37. CH$_2$=CCl$_2$	10.160	9.79								
38. CH$_3$CH=CH$_2$	9.672	9.73								
39. CH$_2$=C(CH$_3$)$_2$	9.280	9.58								
40. CH$_2$=C(CH$_3$)CH=CH$_2$	8.852	8.84								
41. CH$_2$=CH−CH=O	10.113	10.103								
42. CH$_2$=C(CH$_3$)CH=O	10.034	9.92								
43. CH$_2$=C(CN)$_2$	11.871	11.38								
44. CH$_2$=CH−C(O)CH$_3$	9.786	9.64								
45. CH$_3$CH$_2$O−CH=CH$_2$	8.559	8.8								
46. CH$_2$=CH−C(O)NH$_2$	9.909	9.5								
47. CH$_2$=CH−CH$_2$−OH	10.183	9.67								
48. CH$_2$=CH−C$_5$H$_3$N[c]	9.029	8.6								
49. CH$_2$=C(CH$_3$)C(O)OH	10.497	10.15								
50. CH$_2$=CH−OCH$_3$	8.628	8.93								
51. CH$_2$=CHF	10.290	10.363								
52. CF$_2$=CF$_2$	10.413	10.12								
RMSD	0.366		0.064		0.159		0.242		0.846	
R (correlation coefficient)	0.993		0.953		0.987		0.991		0.978	

[a] Experimental IPs and EAs from ref 48 unless indicated otherwise. Experimental electron excitation energies from ref 15 and references therein. [b] Experimental vertical ionization energy for CH$_4$ from ref 49. [c] 2-Vinylpyridine.

the experimental and calculated IPs. By performing a least-squares fit for all of the 52 systems, we obtain an excellent linear correlation relationship between the experimental IPs and each set of the calculated $-\epsilon_{HOMO}$ values, i.e.

$$\text{IP}_{expt} = 1.3042[-\epsilon_{HOMO}(\text{LBS})] + 0.411 \text{ eV} \quad (9)$$

with $R = 0.993$ and RMSD = 0.360 eV and

$$\text{IP}_{expt} = 1.3023(-\epsilon_{HOMO}) + 0.481 \text{ eV} \quad (10)$$

with $R = 0.993$ and RMSD = 0.366 eV. The IP values

determined by eq 10 are listed in Table 3 for comparison with the experimental data. We also found a similar, excellent linear correlation relationship between the directly calculated IPs and $-\epsilon_{HOMO}$ values

$$\text{IP}_{calc} = 1.3124(-\epsilon_{HOMO}) + 0.514 \text{ eV} \quad (11)$$

with $R = 0.989$ and RMSD = 0.454 eV. These linear correlations are shown in Figure 3.

Electron Affinity. Only 10 of the 52 molecules/atoms under consideration have a postitive electron affinity (EA) value as
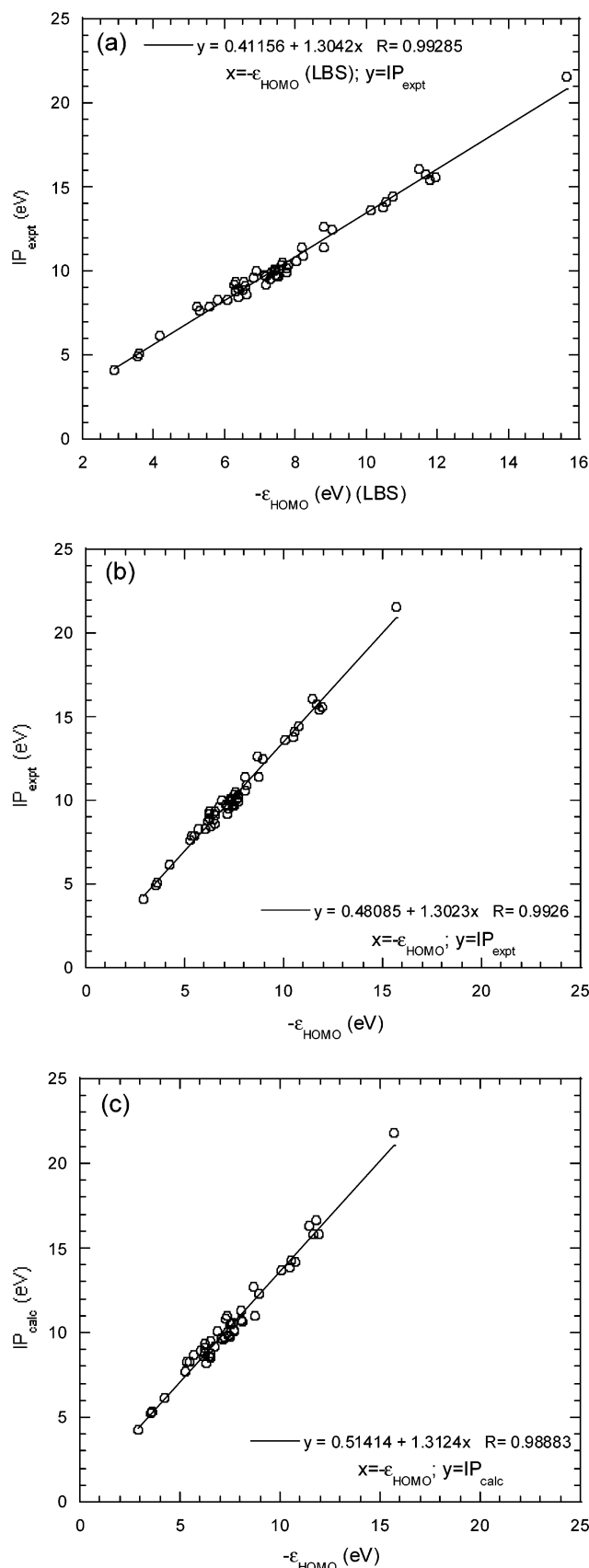
Molecular Properties from DFT Orbital Energies

J. Phys. Chem. A, Vol. 107, No. 20, 2003 **4191**

EAs, and the theory predicts additionally that Li_2 and $CH_2=$ $C(C\equiv N)_2$ will bind an electron. The calculated $-\epsilon_{LUMO}$ values are systematically larger than the corresponding experimental and calculated EAs, but we found a satisfactory linear relationship between the available experimental data and each set of the calculated $-\epsilon_{LUMO}$ values, i.e.

$$EA_{expt} = 0.6580[-\epsilon_{LUMO}(LBS)] - 0.543 \text{ eV} \quad (12)$$

with $R = 0.952$ and RMSD = 0.064 eV and

$$EA_{expt} = 0.6091(-\epsilon_{LUMO}) - 0.475 \text{ eV} \quad (13)$$

with $R = 0.953$ and RMSD = 0.064 eV. For all of the systems whose anionic states are bound, we also found a similar linear relationship between the calculated EA and $-\epsilon_{LUMO}$ values

$$EA_{calc} = 0.4781(-\epsilon_{LUMO}) - 0.213 \text{ eV} \quad (14a)$$

with $R = 0.889$ and RMSD = 0.130 eV. With the larger basis set, we obtained

$$EA_{calc}(LBS) = 0.4583[-\epsilon_{LUMO}(LBS)] - 0.169 \text{ eV} \quad (14b)$$

with $R = 0.927$ and RMSD = 0.099 eV. The low value of R in both cases for the relationship between the LUMO and EA is in part due to the small spread in the values of the EA.

Electronegativity. As noted above, with the finite difference approximation, we have $\chi = (IP + EA)/2$. Thus, we have "experimental" χ values for the 10 systems whose experimental EAs are available. Because the calculated IPs and EAs are all in good agreement with the corresponding experimental IPs and EAs, it is not surprising that the calculated χ values are also in good agreement with the available experimentally derived χ values. In addition, the negative of the calculated average HOMO/LUMO energies, i.e., $\chi_{HL} = -(\epsilon_{HOMO} + \epsilon_{LUMO})/2$, are also close to the experimentally derived and calculated χ values. The reasonable agreement of the calculated χ_{HL} value with χ is due to some cancellation of errors; the calculated $-\epsilon_{HOMO}$ value is systematically smaller than the IP, whereas the calculated $-\epsilon_{LUMO}$ value is systematically larger than the EA. As shown in Figure 5, we found a linear correlation relationship between the available experimentally derived χ values and each set of the calculated χ_{HL} values, i.e.

$$\chi_{expt} = 1.3192\chi_{HL}(LBS) - 0.511 \text{ eV} \quad (15)$$

with $R = 0.986$ and RMSD = 0.167 eV and

$$\chi_{expt} = 1.3207\chi_{HL} - 0.516 \text{ eV} \quad (16)$$

with $R = 0.987$ and RMSD = 0.159 eV. We also found an approximate linear relationship between the calculated χ_{HL} and χ values for all of the 52 systems

$$\chi_{calc} = 1.0590\chi_{HL} + 0.330 \text{ eV} \quad (17)$$

with $R = 0.935$ and RMSD = 0.369 eV. Equation 17 is not as good, as shown in Figure 5c, because χ is derived from both the IP and the EA. The negative EA component is difficult to determine accurately for unbound anionic states as noted above, although the IP component can be determined reliably. Nevertheless, the magnitudes of the absolute EA values are
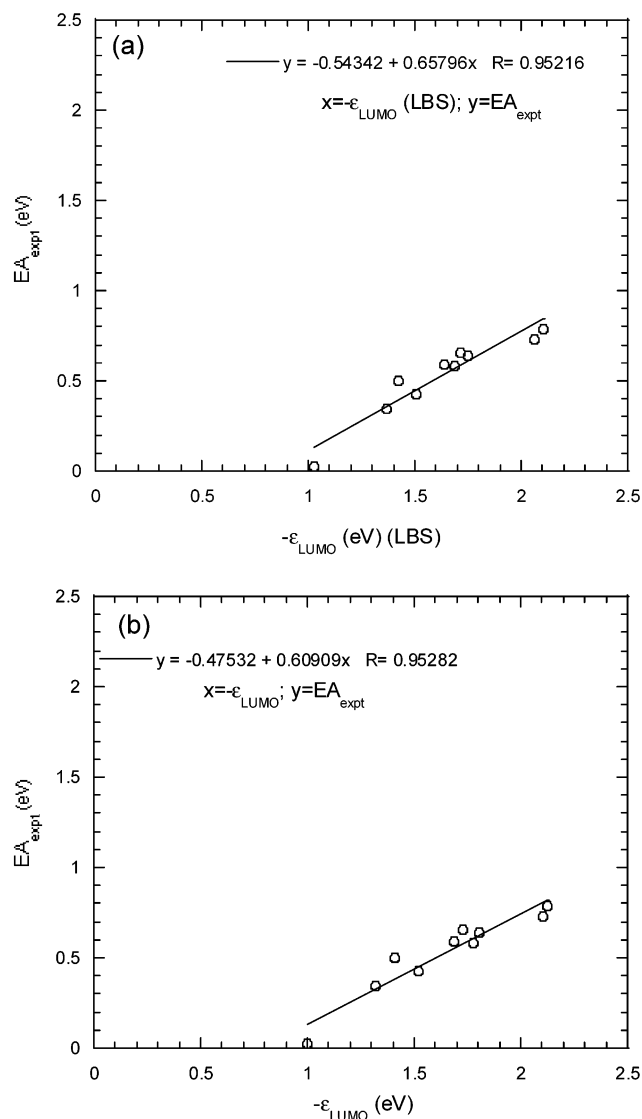
Figure 3. Plot of the experimental (a and b) and calculated (c) ionization potentials versus the $-\epsilon_{HOMO}$ values calculated using the 6-31+G* (b, c) or larger (a) basis set.

identified by experiment. A negative EA value as listed in Table 1 simply means that the anionic state is unbound. The calculated EAs are all in good agreement with the available experimental

Figure 4. Plot of the experimental electron affinities versus the $-\epsilon_{LUMO}$ values calculated using the 6-31+G* (b) and larger (a) basis sets.

generally much smaller than those of the corresponding IP values. Thus, the accuracy of the calculated χ's is dominated by that of the calculated IPs, rather than that of the EAs, giving an overall correlation that is still reasonable.

In addition, there is a satisfactory linear correlation relationship between calculated χ values and the *e* parameter used in the $Q-e$ scheme.[29] Such a linear relationship combined with eq 17 gives a satisfactory linear relationship between the *e* parameter and the calculated χ_{HL} values. The Q parameter used in the $Q-e$ scheme also correlates with the calculated χ_{HL} values and reaction energies. The detailed results for the determination of the Q and *e* parameters have been reported elsewhere.[29]

Hardness. As the electronegativity is the average of the IP and EA, the hardness (η) is also determined by IP and EA, through $\eta = $ IP $-$ EA, based on the finite difference approximation. Thus, we also have "experimental" η values for the same 10 systems. It is not surprising that the DFT-calculated η values are also in good agreement with the available "experimental" η values as shown in Table 1. The calculated HOMO−LUMO energy gaps, i.e., $\eta_{HL} = \epsilon_{LUMO} - \epsilon_{HOMO}$, are systematically smaller than the "experimental"
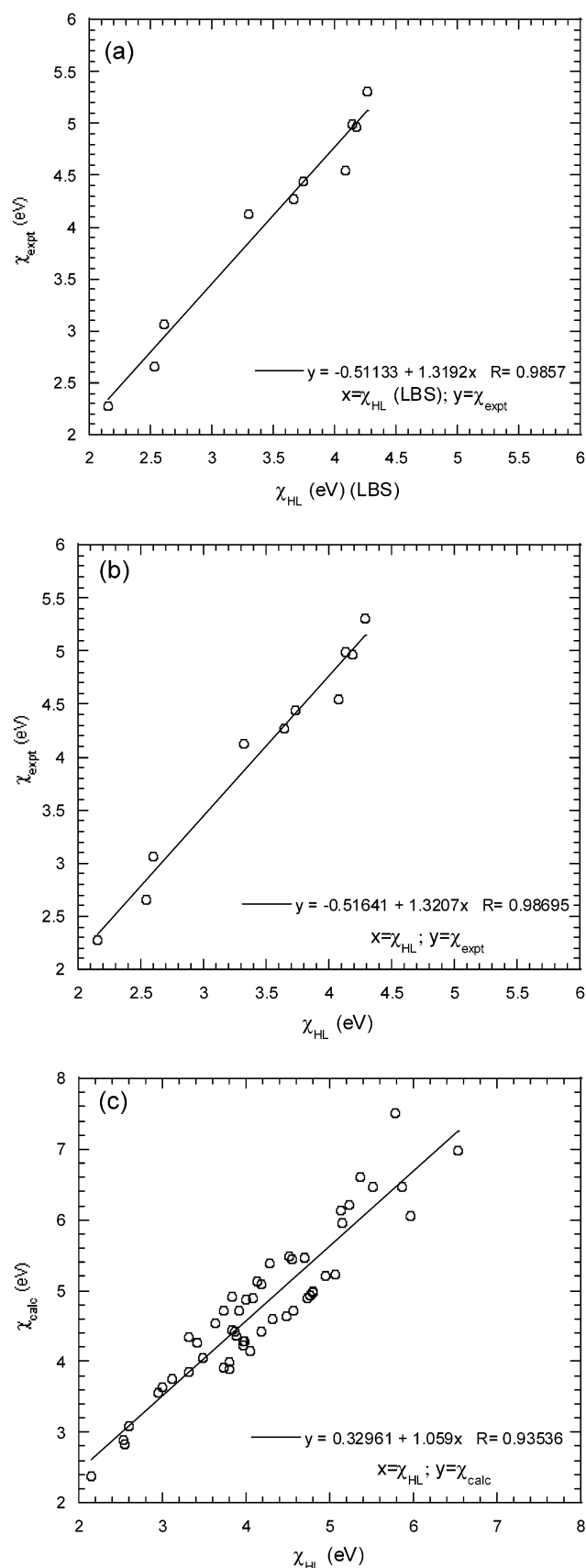

Figure 5. Plot of the experimentally derived (a and b) and calculated (c) electronegativities (χ) versus the χ_{HL} values ($\chi_{HL} = -(\epsilon_{HOMO} + \epsilon_{LUMO})/2$) calculated using the 6-31+G* (b and c) or larger (a) basis set.

and calculated η values. We found an excellent linear relationship between the available "experimental" η values and each

Molecular Properties from DFT Orbital Energies

J. Phys. Chem. A, Vol. 107, No. 20, 2003 **4193**

set of the calculated η_{HL} values, i.e.

$$\eta_{expt} = 1.5724\eta_{HL}(LBS) + 1.282 \text{ eV} \quad (18)$$

with $R = 0.993$ and RMSD = 0.215 eV and

$$\eta_{expt} = 1.6112\eta_{HL} + 1.201 \text{ eV} \quad (19)$$

with $R = 0.991$ and RMSD = 0.242 eV. A similar, satisfactory linear relationship exists between the calculated η_{HL} and η values for all of the 52 systems

$$\eta_{calc} = 1.3343\eta_{HL} + 2.347 \text{ eV} \quad (20)$$

with $R = 0.991$ and RMSD = 0.580 eV. These linear correlations are depicted in Figure 6. The linear correlation between the calculated η_{HL} and η values, i.e., eq 20, is significantly better than that between the calculated χ_{HL} and χ values, i.e., eq 17, for all of the 52 systems, despite the fact that both χ and η are derived from the same IP and EA values. The better linear correlation between the calculated η_{HL} and η values may be partly due to a cancellation of systematic errors in the calculated IP and EA values and also in the calculated HOMO and LUMO energies for the determination of the η_{HL} values.

Electronic Excitation Energy. The experimental first electron excitation energy (τ) is available for 15 systems as shown in Table 1. The results obtained from the TD-DFT calculations are, on the whole, in good agreement with the available experimental data. We can also compare the calculated HOMO−LUMO energy gaps, i.e., $\eta_{HL} = \epsilon_{LUMO} - \epsilon_{HOMO}$, with the available electron excitation energies. As shown in Table 1, the calculated η_{HL} values are systematically larger than the corresponding experimental τ values. A reasonable linear relationship exists between the available experimental τ values and each set of the calculated η_{HL} values:

$$\tau_{expt} = 1.1539\eta_{HL}(LBS) - 2.575 \text{ eV} \quad (21)$$

with $R = 0.961$ and RMSD = 1.138 eV and

$$\tau_{expt} = 0.9269\eta_{HL} - 1.450 \text{ eV} \quad (22)$$

with $R = 0.978$ and RMSD = 0.846 eV. A similar linear relationship exists between the calculated τ and η_{HL} values for all of the 52 systems

$$\tau_{TD} = 0.8616\eta_{HL} - 1.393 \text{ eV} \quad (23)$$

with $R = 0.965$ and RMSD = 0.757 eV. These linear correlations are shown in Figure 7, along with a linear relationship between the experimental and calculated τ_{TD} values

$$\tau_{expt} = 0.9859\tau_{TD} - 0.455 \text{ eV} \quad (24)$$

with R = 0.992 and RMSD = 0.509 eV.

Conclusion

We have performed a series of DFT calculations by using a commonly used exchange-correlation functional, B3LYP, on a variety of representative molecular/atomic systems, including various inorganic and organic molecules with covalent and ionic bonds. The basis set dependence of the DFT results has been examined, particularly for the HOMO and LUMO energies. We obtained a general, nearly perfect linear correlation between the HOMO energies calculated by using the 6-31+G* basis set and
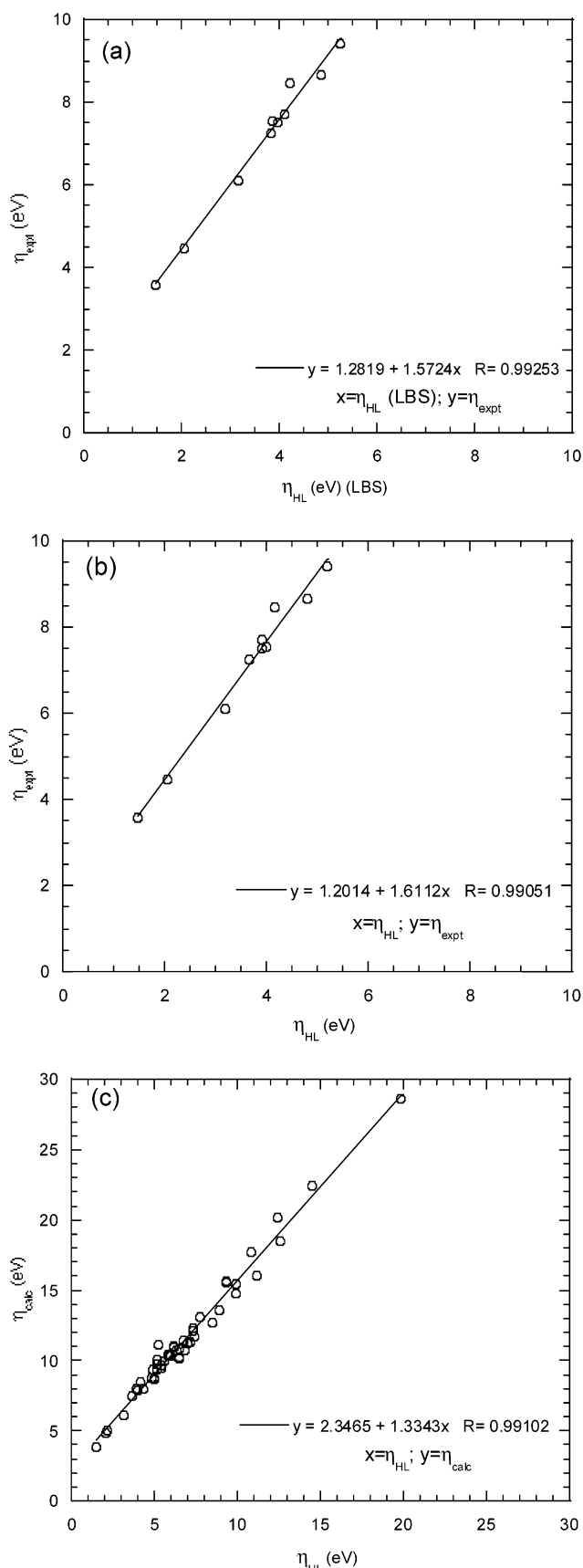

Figure 6. Plot of the experimentally derived (a and b) and calculated (c) hardness (η) values versus the HOMO−LUMO energy gaps (η_{HL}) calculated using the 6-31+G* (b and c) or larger (a) basis set.

those using a much larger basis set (i.e., aug-cc-pVTZ+1). We demonstrated a very simple rule for determining whether a small basis set is adequate or not for calculating the LUMO energy
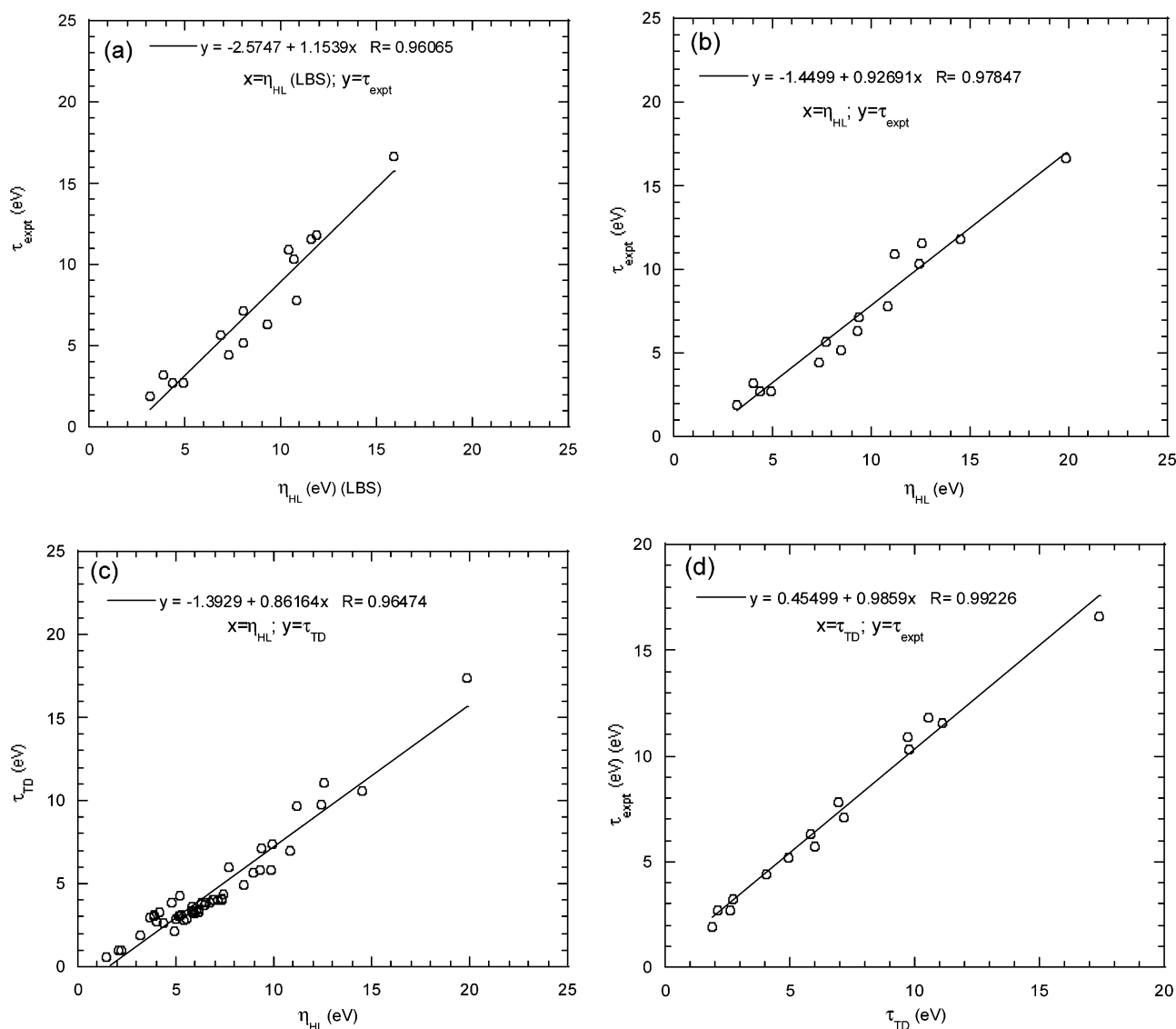
Figure 7. Plots of the experimental (a and b) and calculated (c) first electron excitation energies (τ) versus the HOMO−LUMO energy gaps (η_{HL}) calculated using the 6-31+G* (b and c) or larger (a) basis set, along with a plot (d) of the experimental excitation energies versus the calculated excitation energies.

of a molecule. If the LUMO energy calculated by using the selected basis set is negative then that basis set is appropriate for studying qualitative trends. All of the calculated positive $-\epsilon_{LUMO}$ values (for 41 molecules) show an excellent linear correlation relationship.

The directly calculated ionization potential (IP), electron affinity (EA), electronegativity (χ), hardness (η), and first electron excitation energy (τ) are all in good agreement with the available experimental data. It has been shown that an excellent, generally applicable linear correlation relationship exists between the calculated HOMO energies and experimental/calculated IPs. Satisfactory linear correlation relationships also exist between the calculated LUMO energies and experimental/calculated EAs (for the bound anionic states), between the calculated average HOMO/LUMO energies and χ values, between the calculated HOMO−LUMO energy gaps and η values, and between the calculated HOMO−LUMO energy gaps and experimental/calculated first excitation energies. Based on these linear correlation relationships, the calculated HOMO and LUMO energies can be used to semiquantitatively estimate the ionization potential, electron affinity, electronegativity, hardness, and first excitation energy.

References and Notes

(1) Hohenberg, P.; Kohn, W. *Phys. Rev. B* **1964**, *136*, 864.
(2) Kohn, W.; Sham, L. J. *Phys. Rev. A* **1965**, *140*, 1133.
(3) Parr, R. G.; Yang, W. *Density-Functional Theory of Atoms and Molecules*; Oxford University Press: Oxford, 1989.
(4) Levine, I. N. *Quantum Chemistry*, 5th ed.; Prentice Hall: Englewood Cliffs, NJ, 2000.
(5) Kohn, W. *Rev. Mod. Phys.* **1999**, *71, 1253*, 1999.
(6) Perdew, J. P.; Parr, R. G.; Levy, M.; Balduz, J. L., Jr. *Phys. Rev. Lett.* **1982**, *49*, 1691.
(7) Janak, J. F. *Phys. Rev. B* **1978**, *18*, 7165.
(8) Perdew, J. P.; Levy, M. *Phys. Rev. B* **1997**, *56*, 16021.
(9) Almbladh, C. O.; von Barth, U. *Phys. Rev. B* **1985**, *31*, 3231.

Molecular Properties from DFT Orbital Energies

J. Phys. Chem. A, Vol. 107, No. 20, 2003 **4195**

(10) von Barth, U. In *Many-Body Phenomena at Surface*; Langreth, D. C., Suhl, H., Eds.; Academic Press: New York, 1984.

(11) Katriel, J.; Davidson, E. R. *Proc. Natl. Acad. Sci.* **1980**, *77*, 4403.

(12) Levy, M.; Perdew, J. P.; Sahni, V. *Phys. Rev. A* **1984**, *30*, 2745.

(13) Kleinman, L. *Phys. Rev. B* **1997**, *56*, 12042.

(14) Kleinman, L. *Phys. Rev. B* **1997**, *56*, 16029.

(15) (a) Garza, J.; Fahlstrom, C. A.; Vargas, R.; Nichols, J. A.; Dixon, D. A. "Orbitals from Molecular Orbital and Density Functional Theories for Ionic Systems". In *Reviews in Modern Quanum Chemistry: A Celebration of the Contributions of R. G. Parr*; Sen, K. D., Ed.; World Scientific: Singapore, 2003, Chapter 50, p 1508. (b) Garza, J.; Nichols, J. A.; Dixon, D. A. *J. Chem. Phys.* **2000**, *112*, 1150. (c) Garza, J.; Nichols, J. A.; Dixon, D. A. *J. Chem. Phys.* **2000**, *112*, 7880. (d) Garza, J.; Nichols, J. A.; Dixon, D. A. *J. Chem. Phys.* **2001**, *113*, 6029. (e) Garza, J.; Vargas, R.; Nichols, J. A.; Dixon, D. A. *J. Chem. Phys.* **2001**, *114*, 639.

(16) Tozer, D. J.; Somasundram, K.; Handy, N. *Chem. Phys. Lett.* **1997**, *265*, 614. Gritsenko, O. V.; van Leeuwen, R.; Baerands, E. J. *J. Chem. Phys.* **1996**, *104*, 8535; Krieger, J. B.; Li, Y.; Iafrate, G. J. *Phys. Rev. A* **1992**, *45*, 101.

(17) Politzer, P.; Abu-Awwad, F. *Theor. Chem. Acta* **1998**, *99*, 83.

(18) Arduengo, A. J., III.; Bocks, H.; Chen, H.; Denk, M.; Dixon, D. A.; Green, J. C.; Herrmann, W. A.; Jones, N. L.; Wagner, M.; West, M. *J. Am. Chem. Soc.* **1994**, *116*, 6641.

(19) Politzer, P.; Abu-Awwad, F.; Murray, J. S. *Int. J. Quantum Chem.* **1998**, *69*, 607.

(20) Stowasser, R.; Hoffmann, R. *J. Am. Chem. Soc.* **1999**, *121*, 3414.

(21) Grabo, T.; Gross, E. K. U. *Chem. Phys. Lett.* **1995**, *240*, 141.

(22) Chen, J.; Krieger, J. B.; Li, Y.; Iafrate, G. J. *Phys. Rev. A* **1996**, *54*, 3939.

(23) Rienstra-Kiracofe, J. C.; Tschumper, G. S.; Schaefer, H. F., III.; Nandi, S.; Ellison, G. B. *Chem. Rev.* **2002**, *102*, 231.

(24) Chong, D. P.; Gritsenko, O. V.; Baerends, E. J. *J. Chem. Phys.* **2002**, *116*, 1760.

(25) Stratmann, R. E.; Scuseria, G. E.; Frisch, M. J. *J. Chem. Phys.* **1998**, *109*, 8218.

(26) (a) Matsuzawa, N. N.; Ishitani, A.; Dixon, D. A.; Uda, T. *J. Phys. Chem. A* **2001**, *105*, 4953. (b) Dixon, D. A.; Matsuzawa, N. N.; Ishitani, A.; Uda, T. *Phys. Stat. Sol.* **2001**, *226*, 69.

(27) Dixon, D. A.; Zhan, C.-G. *J. Am. Chem. Soc.* **2002**, *124*, 2744.

(28) (a) Alfrey, T., Jr.; Price, C. C. *J. Polym. Sci.* **1947**, *2*, 101. (b) Rogers, S. C.; Mackrodt, W. C.; Davis, T. P. *Polymer* **1994**, *35*, 1258.

(29) Zhan, C.-G.; Dixon, D. A. *J. Phys. Chem. A* **2002**, *106*, 10311.

(30) Mulliken, R. S. *J. Chem. Phys.* **1934**, *2*, 782.

(31) Parr, R. G.; Pearson, R. G. *J. Am. Chem. Soc.* **1983**, *105*, 7512.

(32) Jenkins, A. D. *J. Polym. Sci. A Polym. Chem.* **1999**, *37*, 113.

(33) (a) Pauling, L. *The Nature of Chemical Bond*, 3rd ed.; Cornell University Press: New York, 1960. (b) Iczkowski, R. P.; Margrave, J. L. *J. Am. Chem. Soc.* **1961**, *83*, 3547. (c) Parr, R. G.; Donnelly, R. A.; Levy, M.; Palke, W. E. *J. Chem. Phys.* **1978**, *68*, 3801.

(34) Sanderson, R. T. *Science* **1955**, *207*, 121.

(35) Sanderson, R. T. *Chemical Bonds and Bond Energy*; Academic Press: New York, 1976.

(36) Sanderson, R. T. *Polar Covalence*; Academic Press: New York, 1983.

(37) Pearson, R. G. *J. Am. Chem. Soc.* **1963**, *85*, 3533.

(38) Pearson, R. G. *Science* **1966**, *151*, 172.

(39) Pearson, R. G. *Chem. Brit.* **1967**, *3*, 103.

(40) Parr, R. G.; Chattaraj, P. K. *J. Am. Chem. Soc.* **1991**, *113*, 1854.

(41) De Luca, G.; Sicilia, E.; Russo, N.; Mineva, T. *J. Am. Chem. Soc.* **2002** *124*, 1494.

(42) De Proft, F.; Geerlings, P. *Chem. Rev.* **2001**, *101*, 1451.

(43) Becke, A. D. *J. Chem. Phys.* **1993**, *98*, 5648. (b) Lee, C.; Yang, W.; Parr, R. G. *Phys. Rev. B* **1988**, *37*, 785. (c) Stephens, P. J.; Devlin, F. J.; Chabalowski, C. F.; Frisch, M. J. *J. Phys. Chem.* **1994**, *98*, 11623.

(44) Hehre, W. J.; Radom, L.; Schleyer, P. v. R.; Pople, J. A. *Ab Initio Molecular Orbital Theory*; John Wiley & Sons: New York, 1987.

(45) Kendall, R. A.; Dunning, T. H., Jr.; Harrison, R. J. *J. Chem. Phys.* **1992**, *96*, 6796.

(46) Basis sets were obtained from the Extensible Computational Chemistry Environment Basis Set Database, Version 1999, as developed and distributed by the Molecular Science Computing Facility, Environmental Molecular Sciences Laboratory which is part of the Pacific Northwest Laboratory, P.O. Box 999, Richland, WA 99352, and funded by the U.S. Department of Energy. The Pacific Northwest Laboratory is a multi-program laboratory operated by Battelle Memorial Institue for the U.S. Department of Energy under contract DE-AC06-76RLO 1830. Contact David Feller for further information.

(47) Frisch, M. J.; Trucks, G. W.; Schlegel, H. B.; Scuseria, G. E.; Robb, M. A.; Cheeseman, J. R.; Zakrzewski, V. G.; Montgomery, J. A., Jr.; Stratmann, R. E.; Burant, J. C.; Dapprich, S.; Millam, J. M.; Daniels, A. D.; Kudin, K. N.; Strain, M. C.; Farkas, O.; Tomasi, J.; Barone, V.; Cossi, M.; Cammi, R.; Mennucci, B.; Pomelli, C.; Adamo, C.; Clifford, S.; Ochterski, J.; Petersson, G. A.; Ayala, P. Y.; Cui, Q.; Morokuma, K.; Malick, D. K.; Rabuck, A. D.; Raghavachari, K.; Foresman, J. B.; Cioslowski, J.; Ortiz, J. V.; Stefanov, B. B.; Liu, G.; Liashenko, A.; Piskorz, P.; Komaromi, I.; Gomperts, R.; Martin, R. L.; Fox, D. J.; Keith, T.; Al-Laham, M. A.; Peng, C. Y.; Nanayakkara, A.; Gonzalez, C.; Challacombe, M.; Gill, P. M. W.; Johnson, B. G.; Chen, W.; Wong, M. W.; Andres, J. L.; Head-Gordon, M.; Replogle, E. S.; Pople, J. A. *Gaussian 98*, revision A.6; Gaussian, Inc.: Pittsburgh, PA, 1998.

(48) Mallard, W. G., Linstrom, P. J., Eds.; *NIST Chemistry WebBook, NIST Standard Reference Database Number 69*; National Institute of Standards and Technology: Gaithersburg, MD, 2001 (*http://webbook.nist-.gov*).

(49) Bierri, G.; Asbrink, L. *J. Electron. Spectrosc. Relat. Phenom.* **1980**, *20*, 149.

(50) Heryadi, D.; Jones, C. T.; Yeager, D. L. *J. Chem. Phys.* **1997**, *107*, 5088.

(51) Porter, A. R.; Al-Mushadani, O. K.; Towler, M. D.; Needs, R. J. *J. Chem. Phys.* **2001**, *114*, 7795.